Enhancing the Forecast of Ocean Physical Variables through Physics Informed Machine Learning in the Santos Estuary, Brazil

Felipe M. Moreno
Escola Politécnica
Universidade de São Paulo
São Paulo, Brazil
felipe.marino.moreno@usp.br

Luiz A. Schiaveto Neto
Escola Politécnica
Universidade de São Paulo
São Paulo, Brazil
luiz.andre.neto@usp.br

Fabio G. Cozman
Escola Politécnica
Universidade de São Paulo
São Paulo, Brazil
0000-0003-4077-4935

Marcelo Dottori
Oceanographic Institute
Universidade de São Paulo
São Paulo, Brazil
mdottori@usp.br

Eduardo A. Tannuri
Escola Politécnica
Universidade de São Paulo
São Paulo, Brazil
eduat@usp.br

***Abstract*—This work aims to improve the forecast of surface currents in the entrance of the Santos estuary in Brazil by applying Quantile Regression Forests (QRF) to estimate the error of the Santos Operational Forecasting System (SOFS), a physics-based numerical model for the region. This was achieved by using in-situ data, measured between 2019 and 2021, associated with historical forecasted data from the SOFS. The use of QRF to correct the SOFS forecasts led to a increase in skill of 0.332 in Mean Absolute Error (MAE) and almost eliminated the bias error of the predicted currents.**

***Index Terms*—Physics-Informed Machine Learning, Current Forecasting, Quantile Regression Forest, Santos Estuary**

I. Introduction

Numerical simulation of physical models is an important tool in predicting properties of water bodies such as estuaries and basins, where economic activities require precise forecasts for planning purposes. Numerical simulations solve partial differential equations of inertia and transport of water properties, and are notoriously sensitive to uncertainties in the boundary conditions, often relying on parameters that cannot be easily measured directly.

One alternative to forecasting by physical models is to resort to machine learning techniques, where a computer automatically finds patterns in past data and uses those patterns to generate forecasts. Because this process does not inherently take into account physical constraints of the domain, it can output unrealistic patterns when faced with conditions never or rarely seem during the training phase.

There has been interest in merging machine learning algorithms with physical models in order to combine the power of machine learning with the already known physics of the domain under study. This combination, often referred to as Model Based Machine Learning or Physics Informed Machine Learning [1], [2], can be used to improve the accuracy of physical models, by learning and correcting the physical model biases and non-modelled dynamics, or to sped up numerical simulations by partially or totally substituting the numerical solution of differential equations while maintaining physical coherency.

This work aims to improve the forecast of currents in the entrance of the Santos estuary in Brazil, by applying machine learning to estimate the residue of a physical model already developed for this region. After a short literature review in Section II, we describe our problem and data in Sections III and IV, and present our solution in Section V. Results and conclusion are presented in Sections VI and VII respectively.

II. Literature Review

Physics-Informed Machine Learning is an emerging field of study that combines machine learning with physical models aiming to extract better results than the ones achievable by using only physical models or machine learning. The use of machine learning algorithms to estimate or correct the error of physical models has successfully been applied in the field of forecasting environmental conditions, as exemplified in the next paragraphs.

Several proposals employ Artificial Neural Networks (ANN) to correct or estimate model errors; some examples are: to estimate global model errors of temperature, pressure,

This work was carried out at the Center for Artificial Intelligence (C4AI-USP), with support by the São Paulo Research Foundation (FAPESP) under grant number 2019/07665-4 and by the IBM Corporation. This work is also supported in part by FAPESP under grant number 2020/16746-5, the Brazilian National Council for Scientific and Technological Development (CNPq) under grant numbers 310127/2020-3, 312180/2018-7, and Coordination for the Improvement of Higher Education Personnel (CAPES). The authors also thank the Santos Marine Pilots for providing crucial data for this research.

wind, and humidity [3], and to reduce temperature forecast errors of physics-based models [4]–[7].

When dealing with forecasts provided in a grid, some approaches resort to Convolutional Neural Networks (CNN), a type of ANN widely used in image recognition tasks, by taking advantage of the CNN capacity of learning spatial patterns. CNNs have been used to improve the forecasted temperatures in the Scandinavian Peninsula using physics-based model forecasts as input, which obtained typical forecast error reduction betwen 20% and 70% [8], CNNs have also been used to estimate forecast error in wind and 500hPa geopotentital height over Europe [9], and to improve forecast of water transport in the atmosphere by post-processing a numerical model [10].

Other machine learning algorithms have been used in the same manner as post-processors for physics-based numerical models. Quantile Regression Forests (QRF) and Support Vector Machines (SVM) have been used to correct the model error for groundwater baseflow in the Republican River in the United States [11]. Random Forests, SVM and Multi-Model Emsemble were used to improve maximum and minimum temperature forecasts in the city of Seoul (South Korea) [7], and Random Forests have been used to improve temperature forecasts in Alpine regions in northern Italy [6].

III. Overview

This work aims to improve the forecasting of superficial water currents in a channel, by applying the architecture in Figure 1, where the machine learning algorithm works as a post-processor block that will learn the error of the physical model output, and when in operation this estimation of the error provided by the post-processor will be added to the physical model output in order to correct it.

The ideas is based in the fact that the physical model does not account for some effects that are difficult to model or are not being measured (such as the river discharge variation due to rain), while a machine learning algorithm may identify patterns in the data and indirectly consider those non modelled effects. The machine learning algorithm we employed is the Quantile Regression Forest (QRF), an algorithm that outputs a prediction and quantile intervals, that can be used to estimate the uncertainty of the prediction.

Our architecture, depicted in Figure 1, is divided in two phases. The first one is the training phase, when the post-processor is trained to predict the physical model error by using historical data accumulated between the years of 2019 and 2021. The second phase is the operational phase, when the post-processor is integrated in the physical model forecasting pipeline and can be used to effectively improve forecasting.

The area of study chosen to apply that architecture is the entrance of the Santos estuary (P1 in Figure 2) in Brazil. The Santos port, located in the estuary, is the busiest port in Brazil; it sees a huge traffic of vessels that will be benefited by better forecasts of the currents in the estuary. It is also a region with ongoing projects that systematically measure and forecast its metocean conditions, providing us with the data needed for the proposed architecture.

The architecture was developed using Python programming language with the Pandas library for data manipulation. Figures were made using MatPlotLib, Sailborn and Windrose libraries. The QRF algorithm used is available in the scikit-garden library. The Wilcoxon test used is available in the scipy library. All code was written in Python notebooks using the Google Colaboratory.

IV. Data and Physical Model

This section describes the physical model used and how the model and measured data were combined in order to obtain a dataset suitable for the training of the post-processor.

A. Physical Model

A physical model in oceanography usually consists of partial differential equations based on the Navier-Stokes equations, with relevant effects added, such as advection (transport of properties by the movement of water), diffusion, friction in the bottom and others. These models are solved numerically, and it is possible to integrate the differential equations in time in order to obtain a forecast. Since the uncertainties in model parameters and boundary conditions are propagated, the forecast accuracy tends to decrease as the forecast horizon is increased.

The equation 1 exemplifies the continuity and Navier-Stokes equations for water velocities $\vec{V} = [u, v, w]$ in a coordinate system where x and y are horizontal coordinates and z is the vertical coordinate, considering Boussinesq approximation hydrostatic pressure and an incompressible fluid. The parameters are the total water column depth H, surface elevation η, Coriolis acceleration f, water density ρ, water reference density ρ_0, gravitational acceleration g, pressure p and stresses $\tau_i = [\tau_{ix}, \tau_{iy}, \tau_{iz}]$ in the direction i due to both shear (such as viscosity and wind stress) and Reynolds stress. The first equation is the continuity equation, and it denotes that the volumetric difference between the water that enters and exits the water column in a point is reflected in a change in surface elevation in that point. The three remaining equations are the Navier-Stokes momentum balance in the three directions, considering advection and Coriolis accelerations in the left side of the equation and pressure gradient, stresses and buoyancy forces in the z direction in the right side.

$$\begin{cases} \int_0^H \frac{\delta u}{\delta x}\delta z + \int_0^H \frac{\delta v}{\delta y}\delta z + \frac{\delta \eta}{\delta t} = 0 \\ \frac{\delta u}{\delta t} + \vec{V}\cdot\nabla u - fv = -\frac{1}{\rho_0}\frac{\delta p}{\delta x} + \frac{1}{\rho_0}\nabla\tau_x \\ \frac{\delta v}{\delta t} + \vec{V}\cdot\nabla v + fu = -\frac{1}{\rho_0}\frac{\delta p}{\delta y} + \frac{1}{\rho_0}\nabla\tau_y \\ \frac{\delta w}{\delta t} + \vec{V}\cdot\nabla w = -\frac{1}{\rho_0}\frac{\delta p}{\delta y} + \frac{1}{\rho_0}\nabla\tau_y - \frac{\rho}{\rho_0 g} \end{cases} \quad (1)$$

The specific physical Model used for this paper is the Santos Operational Forecasting System (SOFS) [12], an automatic forecasting system that solves the hydrodynamic equations

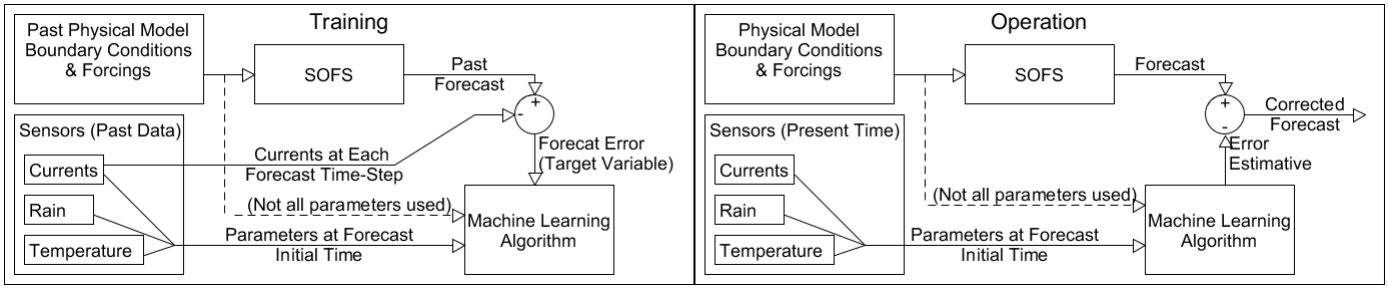

Fig. 1. Proposed architecture for training and for operation of the model.

Fig. 2. Santos Estuary with emphasis on the point of interest for this work (24° 59.608'S,46° 18.006'W). Source: Google Earth.

for the Santos-São Vicente-Bertioga Estuarine System for currents, sea surface height, salinity and temperature. This system is based on the Princeton Ocean Model [13], version POM-rain, and forecasts up to 3 days ahead. The system has two nested grids (Figure 3), for this work we use forecast data from the inner grid.

This model uses atmospheric boundary conditions provided by the Center for Weather Forecasts and Climate Studies (CPTEC, Portuguese acronym) and for tidal boundary conditions they use the seven major astronomical components for the region. Currents in the open boundary are obtained by the Copernicus Marine Environment Monitoring Service Mercator (CMEMS) operated by Mercator Ocean.

The system uses the module POM-rain, which numerically solves the differential equations of the fluid, considering a three-dimensional grid, with sigma vertical coordinates and a curvilinear Arakawa C-grid. Mixing processes are parameterized, and the model is split into an external mode, a faster mode where the 2D equations for entire water column are used, and an internal mode where the 3D equations are used. The internal mode is calculated with a time-step of 4s and the external mode with a time-step of 0.8s.

B. Physical Model Data

The model data that was used to train our machine learning system spawns the period between January 2019 and March 2021, and it contains daily surface current forecasts. The starting time of each forecast is 00:07:30 GMT and it goes up to 21:07:30 GMT of the same day, in steps of 3 hours, adding to 8 steps per daily forecast.

The data was provided originally as NetCDF4 formated files, so the data is converted to the CSV format before being imported to Pandas dataframes for further treatment and

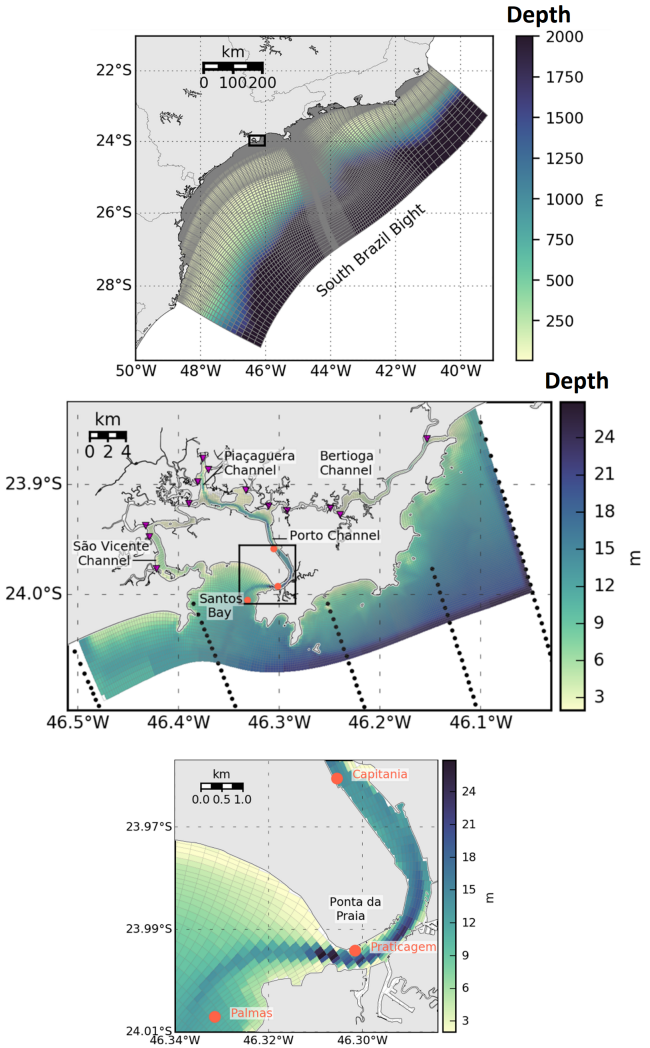

Fig. 3. Coarse (on the top) and fine grids (on the center) of the physical model used, and a detail of the finer grid in Santos Channel (on the bottom) with the point of interest P1 ("Praticagem" in the figure), with bathymetry and scale for reference. Source: Costa et. Al [12]

analysis. Since the data is from a model, there are no gaps or missing data. The currents in the region for the period are shown in Figure 4, it is noticeable that they assume two main directions, one during the flood period and the other during the ebb period.

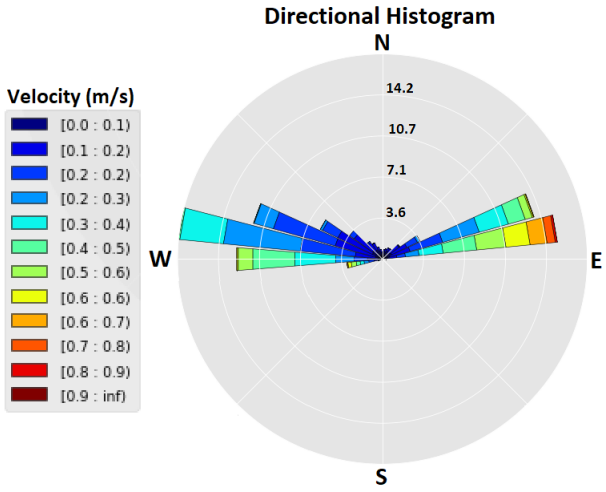

Fig. 4. Directions of the currents in the P1 obtained from the SOFS model (the current direction is the direction where it goes).

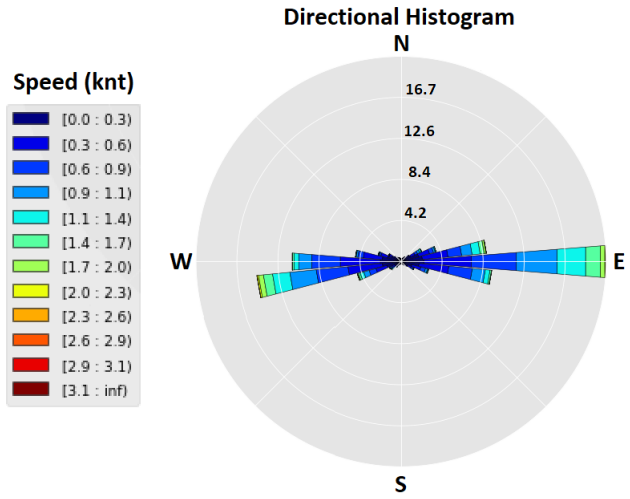

Fig. 5. Directions of the measured currents in the P1. The current direction is the direction where it goes.

The two main directions that the current assumes was used to assign a signal for the current velocity, depending to which main direction the current direction is closest. Negative values mean water is entering the channel, and positive values mean water is being discharged into the estuary by the channel. We also have divided each daily forecast into 8 rows in the dataset, each one containing the date and time of the initial step of the forecast, the current forecast step, and the current predicted by the model. The structure of the dataset is exemplified in Table I.

TABLE I
EXCERPT FROM THE DATASET OF FORECASTS MADE BY THE SOFS.

Forecast Initial Time	Forecast Current Time	Forecast Step	SOFS Current
2019-01-01 00:07:30	2019-01-01 00:07:30	0	0.000
2019-01-01 00:07:30	2019-01-01 03:07:30	1	-0.006
2019-01-01 00:07:30	2019-01-01 06:07:30	2	-0.003
2019-01-01 00:07:30	2019-01-01 09:07:30	3	-0.012
⋮	⋮	⋮	⋮

C. Measurement Data

For the specified point P1 (Figure 2), there are time-series of historical direct measurements (produced by the Santos Marine Pilots) spawning between 2017-2021. These measurements have a periodicity of 5 minutes, consisting of currents in the surface, rainfall, water elevation, waves, winds, and temperature among others. The Santos Marine Pilots also provide in those files a prediction of the water elevation due to astronomical tides. The measurements of currents were 5 minutes averages taken using an Acoustic Doppler current profiler (ADCP) Sontek SL. The currents in the point assume two main directions, entering and exiting the channel (Figure 5). A signal has been attributed to these measured currents in the same manner as in the currents from the SOFS model.

The dataset was provided raw, as text tables in different files for each month, so the data is treated using the Pandas library in Python, where the time-series for each attribute is linearly interpolated in order to obtain the values for the times of forecast in the physical model. Furthermore if there is a gap longer than 180 minutes between the measurements in any of the time-series, the point is not used. All the attributes available have been used, and two derived attributes have been created as well.

The first derived attribute added to the dataset is the hourly rate of change in the measured water level in the point P1, and the second attribute created is the hourly rate of change in the water level, considering astronomical tide forecasting. These two attributes might be important, since the gradient of water level is a primary driver of currents in a channel.

D. Combined Data

By the combination of the model's and measurement's data, we assembled a dataset that contains all the variables needed to run the machine learning algorithm. Each row in that dataset contain a step of forecasting from the SOFS model, as well as the respective measurements taken from the region. The measurements available in each row are from the initial time of the daily forecast (00:07:30 GMT), since we will only have past measurements at the start of the forecast. We obtained 6078 complete rows after removing missing values. An overview of the structure of the main variables of the combined data with its main variables is provided in table II.

V. APPLICATION OF PHYSICS-INFORMED MACHINE LEARNING

The algorithm selected for the post processor is the Quantile Regression Forests (QRF). This method is a variant of Random Forests, which are an ensemble of regression trees. Each regression tree by itself is a weak regressor, but when combined

TABLE II

EXCERPT FROM THE DATASET OF COMBINED DATA SHOWING THE MAIN VARIABLES. MEASURED DATA IS FROM THE START OF THE DAILY FORECAST (FORECAST STEP = 0) WHILE MODEL DATA ARE THE FORECASTED VALUES FOR THE TIME OF THE FORECAST STEP. THE TARGET VARIABLE IS THE ERROR OF THE SOFS MODEL WHEN COMPARED TO REAL MEASURED DATA. SOME MEASURED VARIABLES SUCH AS MAXIMUM AND MINIMUM TEMPERATURE, MAXIMUM AND MINIMUM WIND VELOCITY, WIND DIRECTION, MAXIMUM AND MINIMUM RELATIVE HUMIDITY HAVE BEEN OMITTED FROM THE TABLE DUE TO SIZE CONSTRAINTS.

Measured Data								**Model Data**				Target
Temperature C°	**Relative Humidity** %	**Atm. Press.** hPa	**Wind Speed** m/s	**Precipitation** mm	**Meas. Tide** m	**Tide Variation** m/hour	**Current Vel** m/s	**For. Tide** m	**Forecasted tide Hourly Change** m/hour	**Forecast Step**	**SOFS Current** m/s	**SOFS Error** m/s
26.78	86.25	1008	7.58	0	0.78	0.24	0.25	0.84	0.18	0	0.09	-0.156
26.78	86.25	1008	7.58	0	0.78	0.24	0.25	1.16	-0.04	1	0.08	-0.154
26.78	86.25	1008	7.58	0	0.78	0.24	0.25	0.83	-0.18	2	-0.08	0.255
26.78	86.25	1008	7.58	0	0.78	0.24	0.25	0.55	0.04	3	-0.05	-0.058
⋮	⋮	⋮	⋮	⋮	⋮	⋮	⋮	⋮	⋮	⋮	⋮	⋮

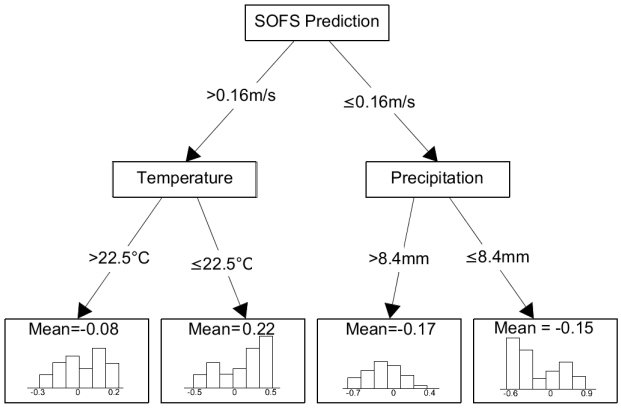

Fig. 6. Example of quantile regression tree with 2 levels. The predicted value is the mean of the target variable of the data that satisfies the split criteria that lead to the end node (leaf node). The distribution of the target values in the leaf node give a percentile interval.

they generate a stronger regressor with better accuracy. A regression tree is a simple regressor that recursively splits the data using one variable at a time as the criterion of the split (Figure 6), until a stop criterion is satisfied. In a random forest the predictions and quantiles of each tree are averaged to generate the QRF prediction.

One of the criteria that lead to the use of regression forests is that it does not generate predictions with values outside of the range of the training set, so when faced with unseen conditions it will not predict unreasonably large values. The selection of QRF is justified because along with the prediction it also provides an estimation of the distribution of the prediction in the form of quantiles, thus allowing the selection of a interval where most likely the prediction lies.

In order to train and test the QRF algorithm, the dataset was randomly divided into two datasets: one is the training dataset, that contains around 75% of the data (4558 rows) and the second is the test dataset containing the remaining rows (1520 rows). Also for the training the Forecast Step column of the dataset was encoded by one-hot-encoding.

To extract the maximum of the algorithm, its hyperparameters must be tuned. The main hyperparameters for the QRF are the number of trees, their depth, the minimum number of elements in a leaf node, the minimum number of elements needed for a split, the maximum number of variables that can be used in one tree, and the loss function. To find the best values for those hyperparameters we employed 5-fold cross-validation over the training dataset. We run a random search with 20 sampled hyperparameters; the hyperparameters that gave the best accuracy were chosen for the training. The selected hyperparameters are shown in Table III.

TABLE III

HYPERPARAMETERS USED TO TRAIN THE QUANTILE REGRESSION FOREST POST-PROCESSOR.

Hyperparameter	**Value**
Maximum tree depth	40
Number of trees	1010
Max. variables per tree	16
Min. no of elements in a leaf node	6
Min. no of elements for split	10
Loss function	Mean Squared Error (MSE)

VI. RESULTS

The performance of the post-processor was evaluated in the holdout dataset containing 25% of the data. The performance of the SOFS is also evaluated in the same dataset and it is used as a baseline. A comparison between the ground truth and the SOFS predictions with, and without the post-processor is provided in Figure 7. In the figure it is possible to notice that the SOFS+QRF is closer or roughly at the same distance to the measured values in most of the cases, but despite this, there are some cases where the SOFS predicted currents are closer to the measured values and the post-processor actually worsens the prediction. In entire test dataset, the post-processor worsens the SOFS prediction in about 30.9% of cases.

To have a wider view of how both prediction methods perform, current histograms were made for both the SOFS and the combination of SOFS+QRF, as provided in Figure 8. When comparing the forecasts provided by the SOFS with the ground truth, it is noticeable that the physical model underestimates the surface current velocity, and underestimates the number of cases where the current is close to zero in the channel.

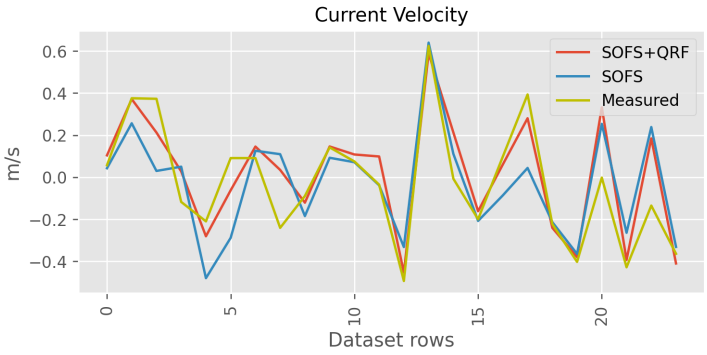

Fig. 7. Time-series of currents forecasted by the SOFS and the SOFS+QRF compared to measured currents for the first 24 rows of the dataset.

The SOFS+QRF generates a histogram much closer to the ground truth, the overall error reduction, when using the post-processor is of 33.2%, the performance for every step of the forecast is shown in Table IV.

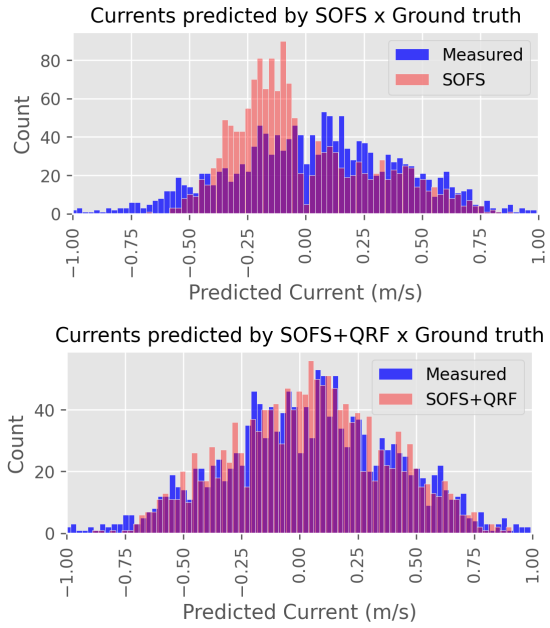

Fig. 8. Histogram of the current predictions for the SOFS and for the combination of SOFS and the QRF post-processor for the holdout dataset versus the measured values. Vertical axis is the number occurrences, horizontal axis is the current velocity.

There is also a remarkable reduction in bias achieved by the use of the post-processor. The distribution of the error is shown in Figure 9, where the difference between the error distributions are evident. The combination of the SOFS+QRF generates an error distribution centered in the zero with narrower spread when compared to the error distribution of the SOFS alone. The bias (mean error) of the SOFS is -0.0565 m/s, while the SOFS+QRF have -0.0018 m/s.

To verify if the error curves are statistically different, a Wilcoxon test is used. The Wilcoxon is a non-parametric

TABLE IV
ABSOLUTE MEAN AND STANDARD DEVIATION ERROR FOR THE SOFS AND THE COMBINATION OF SOFS AND THE QRF PROST-PROCESSOR.

Forecast Step	Current Mean Absolute Velocity Error (Std. Deviation)		
	SOFS	SOFS+QRF	Skill Score (MAE)
+0h	0.148 (0.114)	0.081 (0.0824)	0.455
+3h	0.160 (0.131)	0.119 (0.104)	0.259
+6h	0.188 (0.142)	0.137 (0.106)	0.272
+9h	0.187 (0.138)	0.125 (0.104)	0.331
+12h	0.207 (0.148)	0.135 (0.103)	0.351
+15h	0.142 (0.112)	0.113 (0.0902)	0.203
+18h	0.208 (0.145)	0.135 (0.120)	0.350
+21h	0.203 (0.134)	0.118 (0.103)	0.421

test that is used to reject the null hypothesis that two paired samples have been sampled from the same distribution. The test obtained a p-value of $p = 4$ x10^{-12}, thus indicating that the reduction in error is not likely due to random chance.

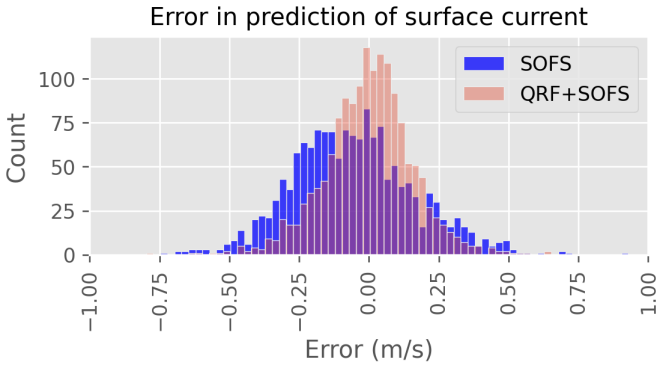

Fig. 9. Histogram of the errors for the SOFS and for the combination of SOFS and the QRF post-processor for the holdout dataset. Vertical axis is the number occurrences, horizontal is error when compared to measured values.

There is also an improvement for cases where the forecast error is large. When using only the SOFS, it is expected that 5% of forecasts will have an error larger than 0.44m/s, and 1% will have an error larger than 0.59m/s, while when using SOFS+QRF 5% of forecasts will have an error larger than 0.32m/s and 1% will have more than 0.47m/s. The maximum forecast error in the dataset is almost the same for both cases, the maximum error in the SOFS forecast was 0.92m/s, and in the SOFS+QRF was 0.80m/s. The quantile interval provided by the QRF is relatively large. When selecting an upper quantile of 97.5% and a lower quantile of 2.5% (thus obtaining a confidence interval where we expect the real error to be contained in 95% of the cases) the average interval obtained is 0.69m/s.

VII. CONCLUSION

In this work we developed and applied an architecture to reduce surface current forecasting errors in the Santos Channel, Brazil, by using Quantile Random Forests (QRF) to estimate and correct the error of a physics-based numerical model (SOFS). The machine learning successfully reduced

bias and increased forecast skill by about 0.332. The use of QRF allowed us to obtain a confidence interval for the forecast, but it was found that this interval is quite large (on average 0,69m/s, for a confidence interval of 95%), which limits its practical use.

As this work is part of an ongoing project in the Santos estuary, the results in this paper provide a comparison baseline for future architectures that are still under development for that region. As future work in the same region, the use of Graph Neural Networks, associated with more data obtained from other measurement stations in the region and numerical models is under study.

REFERENCES

[1] J. Willard, X. Jia, S. Xu, M. Steinbach, and V. Kumar, "Integrating Physics-Based Modeling with Machine Learning: A Survey," vol. 1, no. 1, pp. 1–34, 2020. [Online]. Available: http://arxiv.org/abs/2003.04919

[2] K. Kashinath, M. Mustafa, A. Albert, J. L. Wu, C. Jiang, S. Esmaeilzadeh, K. Azizzadenesheli, R. Wang, A. Chattopadhyay, A. Singh, A. Manepalli, D. Chirila, R. Yu, R. Walters, B. White, H. Xiao, H. A. Tchelepi, P. Marcus, A. Anandkumar, P. Hassanzadeh, and Prabhat, "Physics-informed machine learning: Case studies for weather and climate modelling," 4 2021.

[3] M. Bonavita and P. Laloyaux, "Machine Learning for Model Error Inference and Correction," *Journal of Advances in Modeling Earth Systems*, vol. 12, no. 12, 12 2020.

[4] C. Marzban, "Neural Networks for Post-processing Model Output: ARPS," Tech. Rep., 2002. [Online]. Available: http://www.nhn.ou.edu/

[5] S. Vashani, M. Azadi, and S. Hajjam, "Comparative Evaluation of Different Post Processing Methods for Numerical Prediction of Temperature Forecasts over Iran," *Research Journal of Environmental Sciences*, vol. 4, no. 3, pp. 305–316, 2010. [Online]. Available: www.academicjournals.com

[6] E. Eccel, L. Ghielmi, P. Granitto, R. Barbiero, F. Grazzini, and D. Cesari, "Prediction of minimum temperatures in an alpine region by linear and non-linear post-processing of meteorological models," *Nonlin. Processes Geophys*, vol. 14, pp. 211–222, 2007. [Online]. Available: www.nonlin-processes-geophys.net/14/211/2007/

[7] D. Cho, C. Yoo, J. Im, and D. H. Cha, "Comparative Assessment of Various Machine Learning-Based Bias Correction Methods for Numerical Weather Prediction Model Forecasts of Extreme Air Temperatures in Urban Areas," *Earth and Space Science*, vol. 7, no. 4, 4 2020.

[8] R. Isaksson, "Reduction of Temperature Forecast Errors with Deep Neural Networks," Uppsala, pp. 1–34, 2018.

[9] S. Scher and G. Messori, "Predicting weather forecast uncertainty with machine learning," *Quarterly Journal of the Royal Meteorological Society*, vol. 144, no. 717, pp. 2830–2841, 10 2018.

[10] W. E. Chapman, A. C. Subramanian, L. Delle Monache, S. P. Xie, and F. M. Ralph, "Improving Atmospheric River Forecasts With Machine Learning," *Geophysical Research Letters*, vol. 46, no. 17-18, pp. 10 627–10 635, 9 2019.

[11] T. Xu and A. J. Valocchi, "Data-driven methods to improve baseflow prediction of a regional groundwater model," *Computers and Geosciences*, vol. 85, pp. 124–136, 12 2015.

[12] C. G. Costa, J. R. B. Leite, B. M. Castro, A. F. Blumberg, N. Georgas, M. Dottori, and A. Jordi, "An operational forecasting system for physical processes in the Santos-Sao Vicente-Bertioga Estuarine System, Southeast Brazil," *Ocean Dynamics*, vol. 70, no. 2, pp. 257–271, 2 2020.

[13] A. F. Blumberg and G. L. Mellor, "A Description of a Three-Dimensional Coastal Ocean Circulation Model," in *Three-Dimensional Coastal Ocean Models*. American Geophysical Union (AGU), 1987, pp. 1–16. [Online]. Available: https://agupubs.onlinelibrary.wiley.com/doi/abs/10.1029/CO004p0001